

# Levels of Complexity in Scale-Invariant Neural Signals

Plamen Ch. Ivanov<sup>1</sup>, Jeffrey M. Hausdorff<sup>2</sup>, S. Havlin<sup>3</sup>  
Luís A. Nunes Amaral<sup>1,4</sup>, Kuniharu Arai<sup>5</sup>, Verena Schulte-Frohlinde<sup>1</sup>  
Mitsuru Yoneyama<sup>6,7</sup>, H. Eugene Stanley<sup>1</sup>

<sup>1</sup> Center for Polymer Studies and Department of Physics, Boston University, Boston, MA 02215

<sup>2</sup> Harvard Medical School, Boston, MA 02115 and Tel-Aviv Sourasky Medical Center, Tel-Aviv, Israel

<sup>3</sup> Department of Physics and Gonda-Goldschmied Center for Medical Diagnosis, Bar-Ilan University, Ramat-Gan 52900, Israel

<sup>4</sup> Department of Chemical and Biological Engineering, Northwestern University, Evanston, Illinois 60208

<sup>5</sup> The Smith-Kettlewell Eye Research Institute, San Francisco, CA 94115

<sup>6</sup> Mitsubishi Chemical Group, Science and Technology Center Inc., Yokohama, Japan

<sup>7</sup> Research Institute for Electronic Science, Hokkaido University, Sapporo, Japan

(Dated: August 31, 2018)

Many physical and physiological signals exhibit complex scale-invariant features characterized by  $1/f$  scaling and long-range power-law correlations, suggesting a possibly common control mechanism. Specifically, it has been suggested that dynamical processes influenced by inputs and feedback on multiple time scales may be sufficient to give rise to  $1/f$  scaling and scale invariance. Two examples of physiologic signals that are the output of hierarchical, multi-scale physiologic systems under neural control are the human heartbeat and human gait. Here we show that while both cardiac interbeat interval and gait interstride interval time series under healthy conditions have comparable  $1/f$  scaling, they still may belong to different complexity classes. Our analysis of the magnitude series correlations and multifractal scaling exponents of the fluctuations in these two signals demonstrates that in contrast with the nonlinear multifractal behavior found in healthy heartbeat dynamics, gait time series exhibit less complex, close to monofractal behavior and a low degree of nonlinearity. These findings underscore the limitations of traditional two-point correlation methods in fully characterizing physiologic and physical dynamics. In addition, these results suggest that different mechanisms of control may be responsible for varying levels of complexity observed in physiological systems under neural regulation and in physical systems that possess similar  $1/f$  scaling.

PACS numbers: 05.40+j, 05.45Tr, 87.10.+e, 87.19.Hh, 87.45Dr., 87.23Ge, 87.80.-y, 87.90.+y

## I. INTRODUCTION

Many dynamic systems generate outputs with fluctuations characterized by  $1/f$ -like scaling of the power spectra,  $S(f)$ , where  $f$  is the frequency. These fluctuations are often associated with nonequilibrium dynamic systems possessing multiple degrees of freedom [1, 2], rather than being the output of a classic “homeostatic” process [3–5]. It is generally assumed that the presence of many components interacting over a wide range of time or space scales could be the reason for the  $1/f$  spectrum in the fluctuations [6, 7]. Fluctuations exhibiting  $1/f$ -like behavior are often termed “complex”, since they obey a scaling law indicating a hierarchical fractal organization of their frequency (time scale) components rather than being dominated by a single frequency.  $1/f$  behavior is common in a variety of physical, biological and social systems [7–15]. The ubiquity of the  $1/f$  scale-invariant phenomenon has triggered in recent years the development of generic mechanisms describing complex systems, independent of their particular context, in order to understand the “unifying” features of these systems [16–19].

To answer the question whether fluctuations in signals generated by integrated physiological systems exhibit the same level of complexity, we analyze and compare the time series generated by two physiologic control systems under multiple-component integrated neural control — the human gait and the human heartbeat. We chose these two particular examples because human gait and heartbeat control share certain fundamental properties, e.g., both originate in oscillatory centers.

In the case of the heart, the pacemaker is located in the sinus node in the right atrium [20]. For gait, pacemakers called central pattern generators are thought to be located in the spinal cord [21].

However, these two systems are distinct, suggesting possible dynamical differences in their output. For example, heartbeat fluctuations are primarily controlled by the involuntary (autonomic) nervous system. In contrast, while the spontaneous walking rhythm is an automatic-like process, voluntary inputs play a major role. Further, gait control resides in the basal ganglia and related motor areas of the central nervous system, while the heartbeat is controlled by the sympathetic and parasympathetic branches of the autonomic nervous system [20, 22].

Previous studies show comparable two-point linear correlations and  $1/f$  power spectra in heart rate [23–27] and human gait [28–30], suggesting that differences in physiologic control may not be manifested in beat-to-beat and interstride interval fluctuations. Recent studies focusing on higher order correlations and nonlinear properties show that the human heartbeat exhibits not only  $1/f$  fractal but also multifractal properties [31]. Since multifractal signals require many scaling indices to fully characterize their scaling properties, they may be considered to be more complex than those characterized by a single fractal dimension, such as classical  $1/f$  noise. Although the origins of the multifractal features in heartbeat dynamics are not yet understood, there is evidence that they relate to the complex intrinsic neuroautonomic regulation of the heart [31, 32]. Human gait, e.g., free unconstrained walk-

ing, is also a physiological process regulated by complex hierarchical feedback mechanisms involving supra-spinal inputs [21]. Moreover, recent findings indicate that the scaling properties of gait fluctuations relate to neural centers on the higher supra-spinal level rather than to lower motor neurons or environmental inputs [33, 34]. Thus it would be natural to hypothesize that the fluctuations in healthy unconstrained human gait exhibit similar fractal and multifractal features, and that human gait dynamics may belong to the same “complexity class” as cardiac dynamics.

We employ two techniques — magnitude and sign decomposition analysis [35, 36] and multifractal analysis [37, 38] — to probe long-term nonlinear features, and to compare the levels of complexity in heartbeat and interstride interval fluctuations. To this end, we analyze interstride interval time series from 10 young healthy men (mean age 22 years) with no history of neuromuscular disorders [39]. Subjects walked continuously for 1 hour at a self-selected usual pace on level ground around a flat, obstacle-free, approximately oval, 400m long path. The interstride interval was measured using a ground reaction force sensor — ultra-thin force-sensitive switches were taped inside one shoe and data were recorded on an ambulatory recorder using a previously validated method [40]. We compare the results of our gait analysis with results we have previously obtained [31, 35, 41, 42] from 6-hour long heartbeat interval records from 18 healthy individuals (13 female and 5 male, mean age 34 years) during daily activity (12:00 to 18:00) [39].

As described below, we systematically compare the scaling properties of the fluctuations in human gait with those in the human heartbeat using power spectral analysis, detrended fluctuation analysis (DFA), magnitude and sign decomposition analysis, and wavelet-based multifractal analysis, and we quantify linear and nonlinear features in the data over a range of time scales.

## II. METHODS

### A. Detrended fluctuation analysis (DFA)

The DFA method was developed because conventional fluctuation analyses, such as power spectral, R/S and Hurst analysis cannot be reliably used to study nonstationary data [43, 45, 46]. One advantage of the DFA method is that it allows the detection of long-range power-law correlations in noisy signals with embedded polynomial trends that can mask the true correlations in the fluctuations of a signal. The DFA method has been successfully applied to a wide range of research fields in physics [47–51], biology [43, 52–55], and physiology [56–59].

The DFA method involves the following steps [44]:

(i) Given the original signal  $s(i)$ , where  $i = 1, \dots, N_{max}$  and  $N_{max}$  is the length of the signal, we first form the profile function  $y(k) \equiv \sum_{i=1}^k [s(i) - \langle s \rangle]$ , where  $\langle s \rangle$  is the mean. One can consider the profile  $y(k)$  as the position of a random walk in one dimension after  $k$  steps.

(ii) We divide the profile  $y(k)$  into non-overlapping segments of equal length  $n$ .

(iii) In each segment of length  $n$ , we fit  $y(k)$ , using a polynomial function of order  $\ell$  which represents the polynomial *trend* in that segment. The  $y$  coordinate of the fit line in each segment is denoted by  $y_n(k)$ . Since we use a polynomial fit of order  $\ell$ , we denote the algorithm as DFA- $\ell$ .

(iv) The profile function  $y(k)$  is detrended by subtracting the local trend  $y_n(k)$  in each segment of length  $n$ . In DFA- $\ell$ , trends of order  $\ell - 1$  in the original signal are eliminated. Thus, comparison of the results for different orders of DFA- $\ell$  allows us to estimate the type of polynomial trends in the time series  $s(i)$ .

(v) For a given segment of length  $n$ , the root-mean-square (r.m.s.) fluctuation for this integrated and detrended signal  $s(i)$  is calculated:

$$F(n) \equiv \sqrt{\frac{1}{N_{max}} \sum_{k=1}^{N_{max}} [y(k) - y_n(k)]^2}. \quad (1)$$

(vi) Since we are interested in how  $F(n)$  depends on the segment length, the above computation is repeated for a broad range of scales  $n$ .

A power-law relation between the average root-mean-square fluctuation function  $F(n)$  and the segment length  $n$  indicates the presence of scaling:

$$F(n) \sim n^\alpha. \quad (2)$$

Thus, the DFA method can quantify the temporal organization of the fluctuations in a given signal  $s(i)$  by a single scaling exponent  $\alpha$  — a self-similarity parameter which represents the long-range power-law correlation properties of the signal. If  $\alpha = 0.5$ , there is no correlation and the signal is uncorrelated (white noise); if  $\alpha < 0.5$ , the signal is anti-correlated; if  $\alpha > 0.5$ , the signal is correlated. The larger the value of  $\alpha$ , the stronger the correlations in the signal.

For stationary signals with scale-invariant temporal organization,  $F(n)$  is related to the Fourier power spectrum  $S(f)$  and to the autocorrelation function  $C(n)$ . For such signals,

$$S(f) \sim f^{-\beta}, \text{ where } [\beta = 2\alpha - 1] \quad (3)$$

and  $\alpha$  is the DFA scaling exponent (Eq. 2) [43, 44]. Thus signals with  $1/f$  scaling in the power spectrum (i.e.  $\beta = 1$ ) are characterized by DFA exponent  $\alpha = 1$ . If  $0.5 < \alpha < 1$ , the correlation exponent  $\gamma$  describes the decay of the autocorrelation function [43]:

$$C(n) \equiv \langle s(i)s(i+n) \rangle \sim n^{-\gamma}, \text{ where } [\gamma = 2 - 2\alpha]. \quad (4)$$

### B. Magnitude and sign decomposition method

Fluctuations in the dynamical output of physical and physiological systems can be characterized by their magnitude (absolute value) and their direction (sign). These two quantities

reflect the underlying interactions in a given system — the resulting “force” of these interactions at each moment determines the magnitude and the direction of the fluctuations. Recent studies have shown that signals with identical long-range correlations can differ in the time organization of the magnitude and sign of the fluctuations [35]. To assess the information contained in these fluctuations, the magnitude and sign decomposition method was introduced [35, 36]. This method involves the following steps:

(i) Given the original signal  $s(i)$  we generate the increment series,  $\Delta s(i) \equiv s(i+1) - s(i)$ .

(ii) We decompose the increment series into a magnitude series  $|\Delta s(i)|$  and a sign series  $\text{sgn}(\Delta s(i))$ .

(iii) To avoid artificial trends we subtract from the magnitude and sign series their average.

(iv) We then integrate both magnitude and sign series, because of limitations in the accuracy of the detrended fluctuation analysis method (DFA) for estimating the scaling exponents of anticorrelated signals ( $\alpha < 0.5$ ).

(v) We perform a scaling analysis using 2nd order detrended fluctuation analysis (DFA-2) on the integrated magnitude and sign series.

(vi) To obtain the scaling exponents for the magnitude and sign series we measure the slope of  $F(n)/n$  on a log-log plot, where  $F(n)$  is the root-mean-square fluctuation function obtained using DFA-2, and  $n$  is the scale.

Fluctuations following an identical  $1/f$  scaling law can exhibit different types of correlations for the magnitude and the sign — e.g., a signal with anticorrelated fluctuations can exhibit positive correlations in the magnitude. Positive correlations in the magnitude series indicate that an increment with large magnitude is more likely to be followed by an increment with large magnitude. Anticorrelations in the sign series indicate that a positive increment in the original signal is more likely to be followed by a negative increment. Further, positive power-law correlations in the magnitude series indicate the presence of long-term *nonlinear* features in the original signal, and relate to the width of multifractal spectrum [36]. In contrast the sign series relates to the *linear* properties of the original signal [36]. The magnitude and sign decomposition method is suitable to probe nonlinear properties in short nonstationary signals, such as 1-hour interstride interval time series.

### C. Wavelet-based multifractal analysis

Previously, analyses of the fractal properties of physiologic fluctuations revealed that the behavior of healthy, free-running physiologic systems may often be characterized as  $1/f$ -like [19, 23–27, 29, 34, 40, 60–71]. Monofractal signals (such as classical  $1/f$  noise) are homogeneous, i.e., they have the same scaling properties throughout the entire signal [72–76]. Monofractal signals can therefore be indexed by a single exponent: the Hurst exponent  $H$  [77].

On the other hand, multifractal signals are nonlinear and inhomogeneous with local properties changing with time. Multifractal signals can be decomposed into many subsets charac-

terized by different *local* Hurst exponents  $h$ , which quantify the local singular behavior and relate to the local scaling of the time series. Thus, multifractal signals require many exponents to fully characterize their properties [78–80]. The multifractal approach, a concept introduced in the context of multi-affine functions [81–84], has the potential to describe a wide class of signals more complex than those characterized by a single fractal dimension.

The singular behavior of a signal  $s(t)$  at time  $t_0$  —  $|s(t) - P_n(t)| \sim |t - t_0|^{h(t_0)}$  for  $t \rightarrow t_0$  — is characterized by the local Hurst exponent  $h(t_0)$  where  $n < h(t_0) < n + 1$  and  $P_n(t)$  is a polynomial fit of order  $n$ . To avoid an *ad hoc* choice of the range of time scales over which the local Hurst exponent  $h$  is estimated, and to filter out possible polynomial trends in the data which can mask local singularities, we implement a wavelet-based algorithm [38]. Wavelets are designed to probe time series over a broad range of scales and have recently been successfully used in the analysis of physiological signals [85–93]. In particular, recent studies have shown that the wavelet decomposition reveals a robust self-similar hierarchical organization in heartbeat fluctuations, with bifurcations propagating from large to small scales [42, 94, 95]. To quantify hierarchical cascades in gait dynamics and to avoid inherent numerical instability in the estimate of the local Hurst exponent, we employ a “mean-field” approach — a concept introduced in statistical physics [1] — which allows us to probe the collective behavior of local singularities throughout an entire signal and over a broad range of time scales.

We study the multifractal properties of interstride interval time series by applying the *wavelet transform modulus maxima* (WTMM) method [37, 38, 96] that has been proposed as a mean-field generalized multifractal formalism for fractal signals. We first obtain the wavelet coefficient at time  $t_0$  from the continuous wavelet transform defined as:

$$W_a(t_0) \equiv a^{-1} \sum_{t=1}^N s(t) \psi((t - t_0)/a), \quad (5)$$

where  $s(t)$  is the analyzed time series,  $\psi$  is the analyzing wavelet function,  $a$  is the wavelet scale (i.e., time scale of the analysis), and  $N$  is the number of data points in the time series. For  $\psi$  we use the third derivative of the Gaussian, thus filtering out up to second order polynomial trends in the data. We then choose the modulus of the wavelet coefficients at each point  $t$  in the time series for a fixed wavelet scale  $a$ .

Next, we estimate the partition function

$$Z_q(a) \equiv \sum_i |W_a(t)|^q, \quad (6)$$

where the sum is only over the maxima values of  $|W_a(t)|$ , and the powers  $q$  take on real values. By not summing over the entire set of wavelet transform coefficients along the time series at a given scale  $a$  but only over the wavelet transform modulus maxima, we focus on the fractal structure of the temporal organization of the singularities in the signal [96].

We repeat the procedure for different values of the wavelet scale  $a$  to estimate the scaling behavior

$$Z_q(a) \sim a^{\tau(q)}. \quad (7)$$

In analogy with what occurs in scale-free physical systems, in which phenomena controlled by the same mechanism over multiple time scales are characterized by scale-independent measures, we assume that the scale-independent measures,  $\tau(q)$ , depend only on the underlying mechanism controlling the system. Thus by studying the scaling behavior of  $Z(a, q) \sim a^{\tau(q)}$  we may obtain information about the self-similar (fractal) properties of the mechanism underlying gait control.

For certain values of the powers  $q$ , the exponents  $\tau(q)$  have familiar meanings. In particular,  $\tau(2)$  is related to the scaling exponent of the Fourier power spectra,  $S(f) \sim 1/f^\beta$ , as  $\beta = 2 + \tau(2)$  [38]. For positive  $q$ ,  $Z_q(a)$  reflects the scaling of the large fluctuations and strong singularities in the signal, while for negative  $q$ ,  $Z_q(a)$  reflects the scaling of the small fluctuations and weak singularities [73, 80, 97]. Thus, the scaling exponents  $\tau(q)$  can reveal different aspects of the underlying dynamics.

In the framework of this wavelet-based multifractal formalism,  $\tau(q)$  is the Legendre transform of the singularity spectrum  $D(h)$  defined as the Hausdorff dimension of the set of points  $t$  in the signal  $s(t)$  where the local Hurst exponent is  $h$ . Homogeneous monofractal signals — i.e., signals with a single local Hurst exponent  $h$  — are characterized by linear  $\tau(q)$  spectrum:

$$\tau(q) = qH - 1, \quad (8)$$

where  $H \equiv h = d\tau(q)/dq$  is the global Hurst exponent. On the contrary, a nonlinear  $\tau(q)$  curve is the signature of nonhomogeneous signals that display multifractal properties—i.e.,  $h(t)$  is a varying quantity that depends upon  $t$ .

### III. RESULTS

In Fig. 1 we show two example time series: (i) an interstride interval time series from a typical healthy subject during  $\approx 1$  hour (3,000 steps) of unconstrained normal walking on a level, obstacle-free surface (Fig. 1a) [39]; (ii) consecutive heartbeat intervals from  $\approx 1$  hour (3,000 beats) record of a typical healthy subject during daily activity (Fig. 1b) [39]. Both time series exhibit irregular fluctuations and nonstationary behavior characterized by different local trends; in fact it is difficult to differentiate between the two time series by visual inspection.

We first examine the two-point correlations and scale-invariant behavior of the time series shown in Fig. 1. Power spectra  $S(f)$  of the gait and heartbeat time series (Fig. 2a) indicate that both processes are described by a power-law relation  $S(f) \sim 1/f^\beta$  over more than 2 decades, with exponent  $\beta \approx 1$ . This scaling behavior indicates self-similar (fractal) properties of the data suggestive of an identical level of complexity as quantified by this linear measure. We obtain similar

results for the interstride interval times series from all subjects in our gait database:  $\beta = 0.9 \pm 0.08$  (group mean  $\pm$  std. dev.) in agreement with previous results [34].

#### A. Detrended fluctuation analysis (DFA)

Next, to quantify the degree of correlation in the interstride and heartbeat fluctuations we apply the DFA method, which also provides a linear measure: plots of the root-mean-square fluctuation function  $F(n)$  vs. time scale  $n$  (measured in stride or beat number) from a second-order DFA analysis (DFA-2) [44–46] indicate the presence of long-range power-law correlations in both gait and heartbeat fluctuations (Fig. 2b). The scaling exponent  $\alpha \approx 0.95$  for the heartbeat signal is very close to the exponent  $\alpha \approx 0.9$  for the interstride interval signal, estimated over the scaling range  $6 < n < 600$ . We obtain similar results for the remaining subjects:  $\alpha = 0.87 \pm 0.03$  (group mean  $\pm$  std. dev.) for the gait data and  $\alpha = 1.04 \pm 0.08$  for the heartbeat data, in agreement with [34].

The results of both power spectral analysis and the DFA method indicate that gait and heartbeat time series have similar scale-invariant properties suggesting parallels in the underlying mechanisms of neural regulation.

#### B. Magnitude and sign decomposition method

To probe for long-term nonlinear features in the dynamics of interstride intervals we employ the magnitude and sign decomposition analysis [35, 36]. Previous studies have demonstrated that information about the nonlinear properties of heartbeat dynamics can be quantified by long-range power-

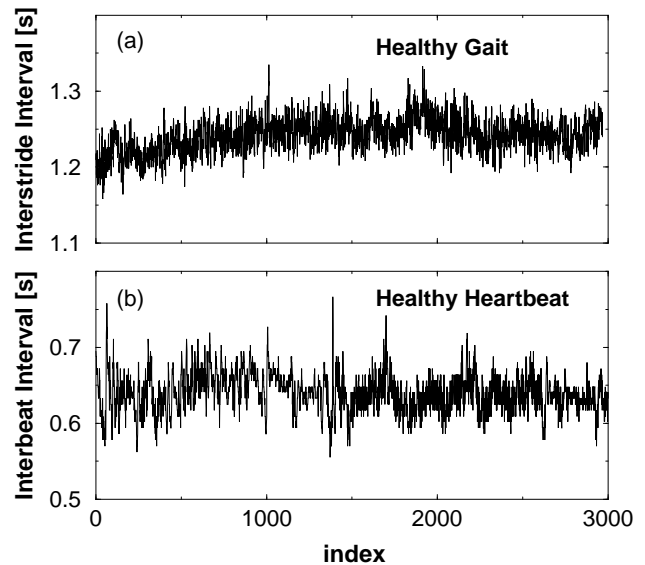


FIG. 1: Representative records of (a) interstride interval time series from a healthy subject and (b) consecutive heartbeat intervals from a healthy subject

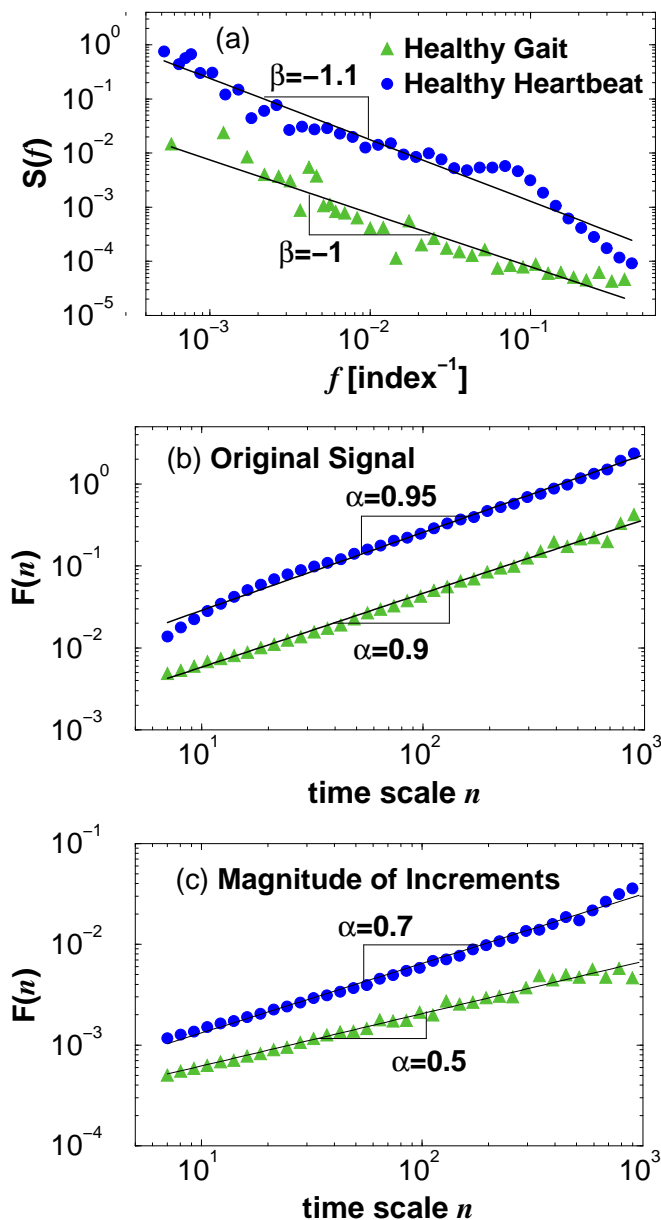


FIG. 2: (a) Power spectra of the gait series ( $\blacktriangle$ ) and heartbeat series ( $\bullet$ ) displayed in Fig. 1. Plots of the root-mean-square fluctuation function  $F(n)$  vs. time scale  $n$  (measured in stride or beat number) from second-order DFA-2 analysis for (b) the interstride and heartbeat interval time series indicating similar power-law correlations, and (c) the magnitude series of the interstride and heartbeat increments showing a surprising difference in the nonlinear properties of the two time series.

law correlations in the magnitude of the increments in heartbeat intervals [35]. Further, correlations in the magnitude are associated with nonlinear features in the underlying dynamics, while linear signals are characterized by an absence of correlations (random behavior) in the magnitude series. To quantify the correlations in the magnitude of the interstride increments we apply the DFA-2 method to the data displayed

in Fig. 1a. Our results show that the magnitude series of the interstride increments exhibits close to random behavior with correlation exponent  $\alpha \approx 0.5$  (denoted by ( $\blacktriangle$ ) in Fig. 2c). In contrast, the magnitude series of the heartbeat increments (Fig. 1b) exhibits strong positive correlations over more than two decades characterized by exponent  $\alpha = 0.7$  (denoted by ( $\bullet$ ) in Fig. 2c). A surrogate test [98, 99] eliminating the nonlinearity in the heartbeat time series by randomizing the Fourier phases but preserving the power spectrum leads to random behavior ( $\alpha = 0.5$ ) in the magnitude series [35]. Thus the striking difference in the magnitude correlations of gait and heartbeat dynamics (both of which are under multilevel neural control) raises the possibility that these two physiologic processes belong to different classes of complexity whereby the neural regulation of the heartbeat is inherently more nonlinear, over a range of time scales, than the neural mechanism of gait control. Our observation of a low degree of nonlinearity in the gait time series is supported by the remaining subjects in the group: over time scales  $6 < n < 600$ , we obtain exponent  $\alpha_{\text{mag}} = 0.57 \pm 0.03$  (group mean  $\pm$  std. dev.) for the gait time series, which is significantly lower than the corresponding exponent  $\alpha_{\text{mag}} = 0.75 \pm 0.06$  obtained for the heartbeat data ( $p = 4.8 \times 10^{-6}$ , by the Student's t-test).

### C. Wavelet-based multifractal analysis

To further test the long-term nonlinear features in gait dynamics we study the multifractal properties of interstride time series. We apply the Wavelet Transform Modulus Maxima (WTMM) method [38, 96] — a “mean-field” type approach to quantify the fractal organization of singularities in the signal. We characterize the multifractal properties of a signal over a broad range of time scales by the multifractal spectrum  $\tau(q)$ .

We first examine the time series shown in Fig. 1. For the gait time series, we obtain a  $\tau(q)$  spectrum which is practically a linear function of the moment  $q$ , suggesting that the gait dynamics exhibit *monofractal* properties (Fig. 3a). This is in contrast with the nonlinear  $\tau(q)$  spectrum for the heartbeat signal (Fig. 3a) which is indicative of multifractal behavior [37, 38]. Further when analyzing the remaining interstride interval recordings we find close to linear  $\tau(q)$  spectra for all subjects in the gait group (Fig. 3b). Calculating the group averaged  $\tau(q)$  spectra we find clear differences: multifractal behavior for the heartbeat dynamics and practically monofractal behavior for the gait dynamics (Fig. 3c). Specifically we find significant differences between the gait and heartbeat  $\tau(q)$  spectra for negative values of the moment  $q$ ; for positive values of  $q$ , the scaling exponents  $\tau(q)$  take on similar values. This is in agreement with the similarity in power spectral and DFA scaling exponents for gait and heartbeat data, which correspond to  $\tau(q = 2)$  (Fig. 2). However, the heartbeat  $\tau(q)$  spectrum is visibly more curved for all moments  $q$  compared with the gait  $\tau(q)$  spectrum which may be approximately fit by a straight line, indicative of a low degree of nonlinearity in the interstride time series. Thus our results show consistent differences between the nonlinear and multifractal properties

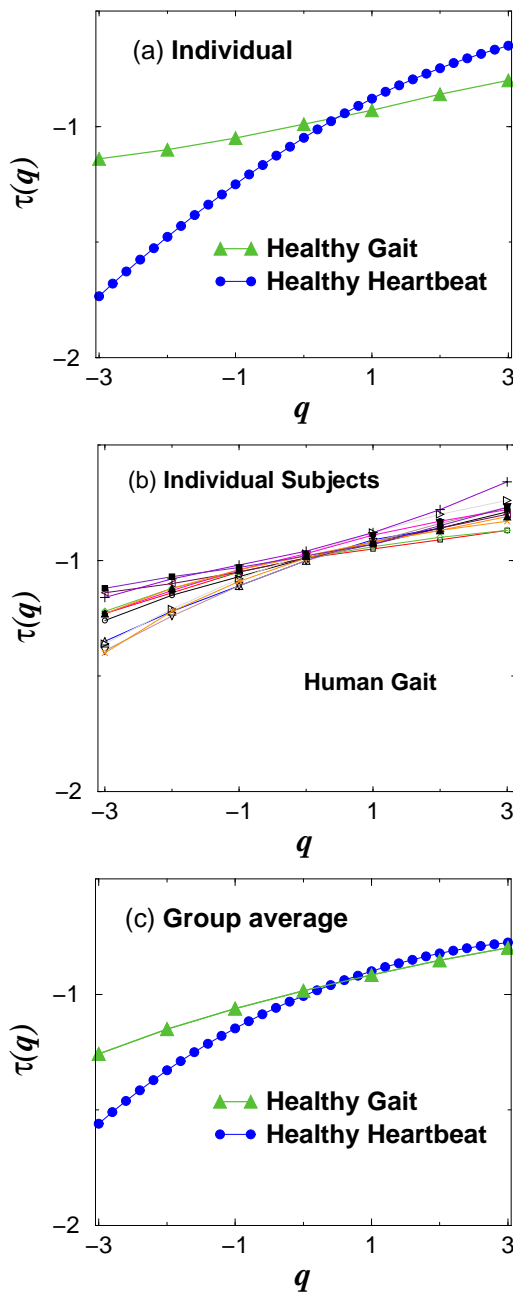


FIG. 3: Multifractal analysis: (a) Multifractal spectrum  $\tau(q)$  for the individual records shown in Fig. 1, where  $\tau$  is a scaling index associated with different moments  $q$  (Eq. 7). A monofractal signal corresponds to a straight line for  $\tau(q)$ , while for multifractal signals  $\tau(q)$  is a nonlinear function of  $q$ . The values of  $\tau(q = 2)$  for both gait and heartbeat time series are very close, in agreement with our findings based on DFA-2 correlation analysis (Fig. 2b). (b) Multifractal spectra  $\tau(q)$  for all ten subjects in our database [39] exhibit close to linear dependence on the moment  $q$ , suggesting monofractal behavior, in contrast to the nonlinear  $\tau(q)$  spectra reported for heartbeat recordings [102]. (c) Group average multifractal spectra  $\tau(q)$  for the gait and heartbeat subjects in our database [39]. The results show a consistent monofractal (almost linear) behavior for the gait time series, in contrast with the multifractal behavior of the heartbeat data.

of gait and heartbeat time series.

Previous studies have shown that reducing the level of physical activity under a constant routine protocol does not change the multifractal features of heartbeat dynamics, while blocking the sympathetic or parasympathetic tone of the neuro-autonomic regulation of the heart dramatically changes the multifractal spectrum, thus suggesting that the observed features in cardiac dynamics arise from the intrinsic mechanisms of control [32]. Similarly, by eliminating polynomial trends in the interstride interval time series corresponding to changes in the gait pace using DFA and wavelet analyses, we find scaling features which remain invariant among individuals. Therefore, since different individuals experience different extrinsic factors, the observed lower degree of nonlinearity as measured by the magnitude scaling exponent and the close-to-monofractal behaviour characterized by practically linear  $\tau(q)$  spectrum appear to be a result of the intrinsic mechanisms of gait regulation. These observations suggest that while both gait and heartbeat dynamics arise from layers of neural control with multiple component interactions, and exhibit temporal organization over multiple time scales, they nonetheless belong to different complexity classes. While both gait and heartbeat dynamics may be a result of competing inputs interacting through multiple feedback loops, differences in the nature of these interactions may be imprinted in their nonlinear and multifractal features: our findings suggest that while these interactions in heartbeat dynamics are of a nonlinear character and are represented by Fourier phase interactions encoded in the magnitude scaling and the multifractal spectrum, feedback mechanisms of gait dynamics lead to decreased interactions among the Fourier phases.

#### D. Further validation of gait results

These new findings are supported by our analysis of a second group of gait subjects. We analyze interstride intervals from an additional group of 7 young healthy subjects (6 male, 1 female, mean age 28 years) recorded using a portable accelerometer [100]. Subjects walked continuously for  $\approx 1$  hour at a self-selected pace on an unconstrained outdoor walking track in a park environment allowing for slight changes in elevation and obstacles related to pedestrian traffic. The stride interval time series in this case were obtained from peak-to-peak intervals in the accelerometer signal output in the direction of the subjects' vertical axis [101]. Compatibility of the ground reaction force sensor used for the gait recordings of the first group [40] with the accelerometer device, and strong correlation between outputs of the two devices was reported in Ref. [100].

We find that for this second group the two-point correlation exponent  $\alpha$ , as measured by the DFA method  $\alpha = 0.90 \pm 0.1$  (group mean  $\pm$  std. dev.) is similar to the group average exponent of the first gait group ( $\alpha = 0.87 \pm 0.03$ ) and also the heartbeat data ( $\alpha = 1.04 \pm 0.08$ ). In contrast, we find again a significantly lower degree of nonlinearity, as measured by the magnitude exponent  $\alpha_{\text{mag}} = 0.62 \pm 0.04$  and the  $\tau(q)$  spectrum, compared with heartbeat dynamics

$\alpha_{\text{mag}} = 0.75 \pm 0.06$  ( $p = 1.3 \times 10^{-3}$ , by the Student's t-test) (Fig. 2c and Fig. 3c). On the other hand, the group averaged value of  $\alpha_{\text{mag}}$  is slightly higher compared with the first gait group ( $\alpha_{\text{mag}} = 0.57 \pm 0.03$ ), and this is associated with slightly stronger curvature in the  $\tau(q)$  spectrum for the second gait group. This may be attributed to the fact that the second group walked in a natural park environment where obstacles, changes in elevation and pedestrian traffic may possibly require the activation of higher neural centers.

The present results are related to a physiologically-based model of gait control where specific interactions between neural centers are considered [12, 13]. In this model a lower degree of nonlinearity (and close-to-linear monofractal  $\tau(q)$  spectrum) reflects increased connectivity between neural centers, typically associated with maturation of gait dynamics in adults. The present results are also consistent with studies that used a different approach to quantify the dynamics of gait, based on estimates of the local Hurst exponents, and reported only weak multifractality in gait dynamics [14, 15].

#### IV. SUMMARY

In summary, we find that while the fluctuations in the output of both gait and heartbeat processes are characterized by

similar two-point correlation properties and  $1/f$ -like spectra, they belong to different classes of complexity — human gait fluctuations exhibit linear and close to monofractal properties characterized by a single scaling exponent, while heartbeat fluctuations exhibit nonlinear multifractal properties which in physical systems have been connected with turbulence and related multiscale phenomena [37, 83, 84, 103].

These findings are of interest because they underscore the limitations of traditional two-point correlation methods in characterizing physiologic and physical time series. In addition, these results suggest that feedback on multiple time scales is not sufficient to explain different types of  $1/f$  scaling and scale-invariance, and highlight the need for the development of new models [104–107] that could account for the scale-invariant outputs of different types of feedback systems.

#### V. ACKNOWLEDGMENTS

We thank Y. Ashkenazy, A.L. Goldberger, Z. Chen, K. Hu and A. Yuen for helpful discussions and technical assistance. This work was supported by grants from NIH/National Center for Research Resources (P41 RR13622), NSF, US-Israel BiNational Science Foundation and Mitsubishi Chemical Co., Yokohama, Japan.

- 
- [1] H.E. Stanley *Introduction to Phase Transitions and Critical Phenomena* (Oxford University Press, New York, 1971).
  - [2] P. Bak and M. Creutz, *Fractals and self-organized criticality. in Fractals in Science*, eds. A. Bunde, and S. Havlin (Springer-Verlag, Berlin, 1994).
  - [3] C. Bernard, *Les Phénomènes de la Vie* (Paris, 1878).
  - [4] B. van der Pol and J. van der Mark, *Phil. Mag* **6**, 763 (1928).
  - [5] W.B. Cannon, *Physiol. Rev.* **9**, 399 (1929).
  - [6] J.B. Johnson, *Phys. Rev.* **26**, 71 (1925).
  - [7] P. Dutta and P.M. Horn, *Rev. Mod. Phys.* **53**, 497 (1981).
  - [8] *Ninth Int. Symp. on Noise in Physical Systems* ed. C. M. Van Vliet (World Scientific, Singapore, 1987).
  - [9] M. Weismann, *Rev. Mod. Phys.* **60**, 537 (1988).
  - [10] T. Musha and H. Higuchi, *Japan. J. Appl. Phys.* **15**, 1271 (1977).
  - [11] Y. Liu, P. Gopikrishnan, P. Cizeau, M. Meyer, C.-K. Peng, H.E. Stanley, *Phys. Rev. E* **60**, 1390-1400 (1999).
  - [12] J. M. Hausdorff, Y. Ashkenazy, C.-K. Peng, P. Ch. Ivanov, H. E. Stanley, A. L. Goldberger *Physica A* **302**, 138 (2001).
  - [13] Y. Ashkenazy, J.M. Hausdorff, P.Ch. Ivanov, H.E. Stanley, *Physica A* **316**, 662 (2002).
  - [14] N. Scafetta, L. Griffin, B. J. West, *Physica A* **328**, 561 (2003).
  - [15] B.J. West and N. Scafetta, *Phys. Rev. E* **67**, 051917 (2003).
  - [16] M.F. Shlesinger, *Ann. NY Acad. Sci.* **504**, 214 (1987).
  - [17] M.F. Shlesinger and B. J. West, in *Random Fluctuations and Pattern Growth: Experiments and Models*, eds. H. E. Stanley and N. Ostrowsky (Kluwer Academics, Boston, 1988).
  - [18] B.J. West and M.F. Shlesinger, *Int. J. Mod. Phys. B* **3**, 795 (1989).
  - [19] J.B. Bassingthwaight, L.S. Liebovitch, and B.J. West, *Fractal Physiology* (Oxford University Press, New York, 1994); L.S. Liebovitch, and T.I. Toth, *Ann. NY Acad. Sci.* **591**, 375 (1990).
  - [20] Berne, R. M. and Levy, M. N. *Cardiovascular Physiology* 6th ed. (C.V. Mosby, St. Louis, 1996).
  - [21] V.T. Inman, H.J. Ralston, and F. Todd, *Human Walking* (Williams and Wilkins, Baltimore, 1981).
  - [22] M. N. Levy, *Circ. Res.* **29**, 437 (1971).
  - [23] M. Kobayashi and T. Musha, *IEEE Trans. Biomed. Eng.* **29**, 456 (1982);
  - [24] Y. Yamamoto and R. L. Hughson, *J. Appl. Physiol.* **71** 1143 (1991).
  - [25] Y. Yamamoto and R. L. Hughson, *Physica D* **68**, 250 (1993).
  - [26] C.K. Peng, J. Mietus, J.M. Hausdorff, S. Havlin, H.E. Stanley, A.L. Goldberger. *Phys. Rev. Lett.* **70**, 1343 (1993).
  - [27] M. Malik and A. J. Camm, eds. *Heart Rate Variability* (Futura, Armonk NY, 1995);
  - [28] M.P. Kadaba, H.K. Ramakrishnan, M.E. Wootten, J. Gainey, G. Gorton, and G.V.B. Cochran, *J. Orthop. Res.* **7**, 849 (1989)
  - [29] J.M. Hausdorff, C.-K. Peng, Z. Ladin, J.Y. Wei, and A.L. Goldberger, *J. Appl. Physiol.* **78**, 349 (1995)
  - [30] H. Yang, F. Zhao, Y. Zhuo, X. Wu, Z. Li. *Physica A* **312**, 23 (2002).
  - [31] P.Ch. Ivanov, L.A.N. Amaral, A. L. Goldberger, S. Havlin, M.G. Rosenblum, Z. Struzik, and H.E. Stanley, *Nature* **399**, 461 (1999).
  - [32] L.A.N. Amaral, P.Ch. Ivanov, N. Aoyagi, I. Hidaka, S. Tomono, A.L. Goldberger, H.E. Stanley, and Y. Yamamoto, *Phys. Rev. Lett.* **86**, 6026 (2001).
  - [33] J.J. Collins and I. Stewart, *Biol. Cybern.* **68**, 287 (1993).
  - [34] J.M. Hausdorff, P.L. Purdon, C.-K. Peng, Z. Ladin, J.Y. Wei, and A.L. Goldberger, *J. Appl. Physiol.* **80**, 1448 (1996).
  - [35] Y. Ashkenazy, P.Ch. Ivanov, S. Havlin, C.-K. Peng, A.L. Goldberger, H.E. Stanley. *Phys. Rev. Lett.* **86**, 1900-1903 (2001).

- [36] Y. Ashkenazy, S. Havlin, P.Ch. Ivanov, C.-K. Peng, V. Schulte-Frohlinde, H.E. Stanley. *Physica A* **323**, 19 (2003).
- [37] J.F. Muzy, E. Bacry, A. Arneodo, *Phys. Rev. Lett.* **67**, 3515 (1991);
- [38] J. F. Muzy, E. Bacry, and A. Arneodo, *Int. J. Bifurc. Chaos* **4**, 245 (1994).
- [39] Gait Database available at <http://www.physionet.org/>; MIT-BIH Normal Sinus Rhythm Database available at <http://www.physionet.org/physiobank/database/ecg>
- [40] J. M. Hausdorff, Z. Ladin, and J. Y. Wei, *J. Biomech.* **28**, 347–351 (1995).
- [41] P.Ch. Ivanov, A. Bunde, L.A.N. Amaral, S. Havlin, J. Fritsch-Yelle, R.M. Baeovsky, H.E. Stanley, A.L. Goldberger. *Europhys. Lett.* **48**, 594 (1999).
- [42] P.Ch. Ivanov, L.A.N. Amaral, A.L. Goldberger, S. Havlin, M.G. Rosenblum, H.E. Stanley, Z. Struzik, *Chaos* **11**, 641 (2001).
- [43] C.-K. Peng, S.V. Buldyrev, A.L. Goldberger, S. Havlin, M. Simons, and H.E. Stanley, *Phys. Rev. E* **47**, 3730 (1993).
- [44] C.-K. Peng, S.V. Buldyrev, S. Havlin, M. Simons, H.E. Stanley, and A.L. Goldberger, *Phys. Rev. E* **49**, 1685 (1994).
- [45] K. Hu, P.Ch. Ivanov, Z. Chen, P. Carpena, H.E. Stanley *Phys. Rev. E* **64**(1), 011114(19) (2001).
- [46] Z. Chen, P.Ch. Ivanov, K. Hu, H.E. Stanley. *Phys. Rev. E* **65**, 041107(15) (2002).
- [47] J. W. Kantelhardt, R. Berkovits, S. Havlin, and A. Bunde, *Physica A* **266**, 461 (1999).
- [48] N. Vandewalle, M. Ausloos, M. Houssa, P. W. Mertens, and M. M. Heyns, *Appl. Phys. Lett.* **74** 1579 (1999).
- [49] K. Ivanova and M. Ausloos, *Physica A* **274**, 349 (1999).
- [50] A. Montanari, R. Rosso, and M. S. Taqqu, *Water Resour. Res.* **36**, (5) 1249 (2000).
- [51] B.D. Malamud and D.L. Turcotte, *J. Stat. Plan. Infer.* **80**, 173 (1999).
- [52] S. V. Buldyrev, A. L. Goldberger, S. Havlin, C.-K. Peng, H.E. Stanley, and M. Simons, *Biophys. J.* **65**, 2673 (1993).
- [53] S.M. Ossadnik, S.B. Buldyrev, A.L. Goldberger, S. Havlin, R.N. Mantegna, C.-K. Peng, M. Simons, and H.E. Stanley, *Biophys. J.* **67**, 64 (1994).
- [54] M.S. Taqqu, V. Teverovsky, and W. Willinger, *Fractals* **3** 785 (1995).
- [55] S. Havlin, S.V. Buldyrev, A.L. Goldberger, R.N. Mantegna, C.-K. Peng, M. Simons, and H.E. Stanley, *Fractals* **3**, 269 (1995).
- [56] N. Iyengar, C.-K. Peng, R. Morin, A. L. Goldberger, and L.A. Lipsitz, *A.M. J. Physiol-Reg. I* **40**, R1078 (1996).
- [57] T. H. Makikallio, J. Koistinen, L. Jordaens, M.P. Tulppo, N. Wood, B. Golosarsky, C.-K. Peng, A.L. Goldberger, H.V. Huikuri, *Am. J. Cardiol.* **83**, 880 (1999).
- [58] A. Bunde, S. Havlin, J.W. Kantelhardt, T. Penzel, J.H. Peter, and K. Voigt, *Phys. Rev. Lett.* **85**, 3736 (2000).
- [59] T.T. Laitio, H.V. Huikuri, E.S.H. Kentala, T.H. Makikallio, J.R. Jalonen, H. Helenius, K. Sariola-Heinonen, S. Yli-Mayry, and H. Scheinin, *Anesthesiology* **93**, 69 (2000).
- [60] R. I. Kitney and O. Rempelman, *The Study of Heart-Rate Variability* (Oxford University Press, London, 1980).
- [61] R.I. Kitney D. Linkens, A.C. Selman, and A.A. McDonald, *Automedica* **4**, 141 (1982);
- [62] L. S. Liebovitch, *Adv. Chem. Ser.* **235**, 357 (1994).
- [63] J. Kurths, A. Voss, P. Saparin, A. Witt, H.J. Kleiner, and N. Wessel, *Chaos* **5**, 88 (1995).
- [64] A.L. Goldberger, *Lancet* **347**, 1312 (1996).
- [65] Y. Q. Chen, M. Z. Ding, and J. A. S. Kelso, *Phys. Rev. Lett.* **79**, 4501 (1997).
- [66] B. J. West and L. Griffin, *Fractals* **6**, 101 (1998).
- [67] S. B. Lowen, L. S. Liebovitch, J. A. White, *Phys. Rev. E* **59**, 5970 (1999).
- [68] S. Havlin, S. V. Buldyrev, A. Bunde, A. L. Goldberger, P. Ch. Ivanov, C.-K. Peng, and H. E. Stanley, *Physica A* **273**, 46 (1999).
- [69] L. Griffin, D. J. West, and B. J. West, *J. Biol. Phys.* **26**, 185 (2000).
- [70] H. E. Stanley, L. A. N. Amaral, P. Gopikrishnan, P. Ch. Ivanov, T. H. Keitt, and V. Plerou, *Physica A* **281**, 60 (2000).
- [71] L. A. Protsman, H. Meeuwsen, P. Hamilton, B. J. West, and J. Wilkerson, *J. Sport & Exercise Psychol.* **23** S67 (2001).
- [72] A. Bunde and S. Havlin, eds., *Fractals and Disordered Systems, Second Edition* (Springer-Verlag, Berlin, 1996).
- [73] H. Takayasu, *Fractals in the Physical Sciences* (Manchester University Press, Manchester UK, 1997).
- [74] T. G. Dewey, *Fractals in Molecular Biophysics* (Oxford University Press, Oxford, 1997).
- [75] A.-L. Barabási and H. E. Stanley, *Fractal Concepts in Surface Growth* (Cambridge University Press, Cambridge, 1995).
- [76] S. Stoev, V. Pipiras, and M. S. Taqqu, *Signal Process* **82j**, 1873 (2002).
- [77] H. E. Hurst, *Trans. Am. Soc. Civ. Eng.* **116** 770 (1951).
- [78] H. E. Stanley and P. Meakin, *Nature* **335** 405 (1988).
- [79] P. Meakin, *Fractals, scaling and growth far from equilibrium* (Cambridge University Press, Cambridge, 1997).
- [80] J. Feder, *Fractals* (Plenum, New York, 1988).
- [81] T. Vicsek and A.-L. Barabási, *J. Phys. A: Math. Gen.* **24** L845 (1991).
- [82] A.-L. Barabasi, P. Szeffalussy, and T. Vicsek, *Physica A* **178** 17 (1991).
- [83] J. Nittmann, G. Daccord, and H.E. Stanley, *Nature* **314**, 141 (1985).
- [84] C. Meneveau and K.R. Sreenivasan, *Phys. Rev. Lett.* **59**, 1424 (1987);
- [85] C. Li and C. Zheng, *Proc. Annu. Conf. on Eng. in Med. and Biol.* **15**, 330 (1993).
- [86] O. Meste, H. Rix, P. Caminal and N. V. Thakor, *IEEE Trans. Biomed. Eng.* **41** 625 (1994).
- [87] L. Senhadji, G. Carrault, J. J. Bellanger and G. Passariello, *IEEE Eng. in Med. and Biol. Mag.* **14**, 167 (1995).
- [88] M. Karrakchou, C. V. Lambrecht and M. Kunt, *IEEE Eng. in Med. and Biol. Mag.* **14**, 179–185 (1995).
- [89] N. V. Thakor, X. R. Guo, Y. C. Sun and D. F. Hanley, *IEEE Trans. Biomed. Eng.* **40**, 1085 (1993).
- [90] D. Morlet, J. P. Couderc, P. Touboul and P. Rubel, *Int. J. Biomed. Comput.* **39**, 311 (1995).
- [91] D. Morlet, F. Peyrin, P. Desseigne, P. Touboul and P. Rubel, *J. Electrocardiol.* **26**, 311 (1993).
- [92] L. Reinhardt, M. Mäkijärvi, T. Fetsch, J. Montonen, G. Sierra, A. Martínez-Rubio, T. Katila, M. Borggreffe and G. Breithardt, *J. Am. Coll. Cardiol.* **27**, 53 (1996).
- [93] M. Karrakchou and M. Kunt, *Ann. Biomed. Eng.* **23**, 562 (1995).
- [94] P. Ch. Ivanov, M. G. Rosenblum, C.-K. Peng, J. Mietus, S. Havlin, H. E. Stanley, and A. L. Goldberger, *Nature* **383**, 323 (1996).
- [95] P. Ch. Ivanov, M. G. Rosenblum, C-K Peng, J. Mietus, S. Havlin, H. E. Stanley, and A. L. Goldberger, *Physica A* **249**, 587 (1998).
- [96] J. F. Muzy, E. Bacry, and A. Arneodo, *Phys. Rev. E* **47**, 875 (1993).
- [97] Vicsek, T. *Fractal Growth Phenomena*, 2nd ed. (World Scientific, Singapore, 1993).



- [98] D. Panter, *Modulation, noise and spectral analysis* (McGraw-Hill, New York, 1965).
- [99] J. Theiler, S. Eubank, A. Longtin, B. Galdrikian, and D. J. Garner, *Physica D* **58**, 77 (1992).
- [100] N. Tanaka, S. Sonoda, Y. Muraoka, Y. Tomita, and N. Chino. *Jpn. J. Rehabil. Med.* **33**, 549 (1996).
- [101] The accelerometer device we used ( $9 \times 6 \times 2\text{cm}$ , weight  $140\text{g}$ ) was developed by Sharp Co. The device, attached to subjects' back, measures the vertical and anteroposterior acceleration profile during walking. The output signals are digitized at a sampling frequency of,  $10^3\text{Hz}$ , and are stored on a memory card. When the subjects' heel strikes the ground a clear peak in the acceleration along the vertical axis is recorded. The positions of these peaks in time are also controlled and verified independently through matching steepest points in the anteroposterior acceleration signal output.
- [102] H.E. Stanley, L.A.N. Amaral, A.L. Goldberger, S. Havlin, P.Ch. Ivanov, C.-K. Peng, *Physica A* **270**, 309 (1999).
- [103] U. Frisch, *Turbulence* (Cambridge University Press, Cambridge UK, 1995).
- [104] P.Ch. Ivanov, L.A.N. Amaral, A.L. Goldberger, H.E. Stanley, *Europhys. Lett.* **43**, 363 (1998).
- [105] D.C. Lin, R.L. Hughson, *Phys. Rev. Lett.* **86**, 1650 (2001).
- [106] P.V.E. McClintock, A. Stefanovska, *Physica A* **314**, 69 (2002).
- [107] R. Yulmetyev, P. Hanggi, F. Gafarov, *Phys. Rev. E* **65**, 046107 (2002).